Spectral transverse instabilities and soliton dynamics in the higher-order multidimensional nonlinear Schrödinger equation

Justin T. Cole, Ziad H. Musslimani

Department of Mathematics, Florida State University, Tallahassee, Florida 32306-4510, USA

Abstract

Spectral transverse instabilities of one-dimensional solitary wave solutions to the two-dimensional nonlinear Schrödinger (NLS) equation with fourth-order dispersion subject to higher-dimensional perturbations are studied. A linear boundary value problem governing the evolution of the transverse perturbations is derived. The eigenvalues of the perturbations are numerically computed using Fourier and finite difference differentiation matrices. It is found that for both signs of the higher-order dispersion coefficient there exists a finite band of unstable transverse modes. In the long wavelength limit we derive an asymptotic formula for the perturbation growth rate that agrees well with the numerical findings. Using a variational formulation based on Lagrangian model reduction, an approximate expression for the perturbation eigenvalues is obtained and its validity is compared with both the asymptotic and numerical results. The time dynamics of a one-dimensional soliton stripe in the presence of a transverse perturbation is studied using direct numerical simulations. Numerical nonlinear stability analysis is also addressed.

Keywords: higher-order dispersion, line solitons, transverse instability

1. Introduction

Solitons, or solitary waves, are self-trapped nonlinear modes that exist in many branches of science such as optics [1, 2, 3, 4, 5], fluid mechanics [6], plasmas [7], ultracold gases [8] biology and chemistry [9, 10]. Among the most intriguing and physically relevant properties associated with these solitary waves is the development of symmetry-breaking instabilities that often lead to the generation of complex nonlinear coherent structures [11].

Modulational instability (MI) is an important example of a symmetry-breaking instability where a constant (in space) amplitude and time-harmonic solution to the underlying governing equation of motion breaks up due to the exponential growth of small modulated perturbations under the combined effects of dispersion and nonlinearity. It was first identified in fluid mechanics [12] and plasma physics [13] and subsequently reported in many other areas of physics [14, 15], particularly in nonlinear optics [16, 17, 18, 19, 20, 21]. Very recently [24], modulational instability of constant amplitude waves for the PT-symmetric NLS equation [22, 23] has also been studied.

Another physically relevant modulational instability process is the so-called transverse instability (TI) (see reviews [25, 26, 27]). Contrary to the "conventional" MI (where the base state is constant in all space dimensions), TI describes the break up of a line soliton (a two-dimensional nonlinear mode localized in one space dimension and uniform in the other) due to the exponential growth of unstable perturbations in the transverse direction. Mathematically speaking, it was first discovered by Zakharov and Rubenchik [28] for the attractive two-dimensional nonlinear Schrödinger equation. They derived an asymptotic expression for the perturbation eigenvalue valid in the long wavelength limit and found that one-dimensional line soliton solutions are transversally unstable. The long time dynamics of the soliton evolution under transverse perturbations is the formation of a train of two-dimensional localized filaments. A similar situation holds for the two-dimensional repulsive (self-defocusing) NLS equation: a dark soliton stripe becomes unstable against random transverse perturbations and disintegrates into a sequence of vortices (snake-type instability) [29, 30, 31]. Transverse instabilities of vector solitons have also been studied theoretically [33, 34, 35]. Experimental observation of TI has been reported in the literature for both the scalar and vector cases [39, 40]. We point out that TI has also been studied in other settings [36], most notably for the hyperbolic NLS equation [37, 38].

Most of the mathematical models used to study MI and TI processes are based on nonlinear, dispersive and conservative evolution equations with the nonlinear Schrödinger equation being a prototypical example [6]. However, higher-order dispersion terms become important in certain special regimes. Specifically, fourth-order dispersion has been demonstrated to play an important role in fiber

Email addresses: jcole@math.fsu.edu (Justin T. Cole), muslimani@math.fsu.edu (Ziad H. Musslimani)

optics [41, 42]. Additionally, modulational instability in NLS-type models with high-order dispersion have been extensively investigated [43, 44, 45, 46, 47, 48].

In this paper, we study spectral transverse instabilities of one-dimensional localized solitary waves subject to two-dimensional perturbations. The model equation considered is based on the two-dimensional nonlinear Schrödinger equation in the presence of a higher-order dispersion

$$i\phi_t + \frac{1}{2}\Delta\phi - \beta\Delta^2\phi + \gamma\left|\phi\right|^2\phi = 0\ , \tag{1}$$

where ϕ is a complex-valued envelope function, β is a real dispersion coefficient, $\gamma = \pm 1$, Δ is the two-dimensional Laplacian describing dispersion in the (x, y) plane and Δ^2 is the so-called bi-Laplacian. When $\beta = 0$, Eq. (1) successfully models several physical phenomena related to optics [2, 6], Bose-Einstein condensates [49], and fluid mechanics [50]. For nonzero β, Eq. (1) can be viewed as a special case of the more general complex Swift-Hohenberg equation derived in [51] as a model of optical wave propagation in a cavity near the onset of lasing. A linear evolution equation for the transverse perturbation is obtained. Using separation of variables, we find an eigenvalue system whose spectrum is numerically computed with the help of differentiation matrices. It is found that when β is positive there exists a finite band of unstable transverse modes and the soliton stripe is unstable against perturbations with small wavenumbers. This long wavelength instability seems to disappear when the higher-order dispersion coefficient β is negative for solitons with small amplitude. In the long wavelength limit we derive an asymptotic formula for the perturbation growth rate that agrees well with the numerical findings. This perturbative result generalizes the formula obtained by Zakharov and Rubenchik [28] for the "classical" two-dimensional nonlinear Schrödinger equation ($\beta = 0$). Based on a variational approach, an approximate expression for the perturbation eigenvalues is also obtained and its validity is compared with the asymptotics as well as the numerical results. The time dynamics of the soliton stripe superimposed with a transverse perturbation is investigated by numerically solving the Cauchy problem associated with Eq. (1). Finally, numerical nonlinear stability results are also presented.

The outline of the paper is as follows. In section 2 we identify families of one-dimensional line soliton solutions followed by (Sec. 3) a thorough analysis of their linear stability. In Secs. 4 and 5 we report on analytical results for the linear stability analysis. Comparison with direct simulations is presented in section 6. We conclude the discussion in section 7.

2. Line (stripe) solitons

We start the discussion by considering a family of one-dimensional soliton solutions to Eq. (1) that are independent of the transverse coordinate y

$$\phi(x, y, t) = \psi(x, \mu)e^{i\mu t}\ , \tag{2}$$

which satisfy the nonlinear boundary value problem

$$\frac{1}{2}\partial_x^2\psi - \beta\partial_x^4\psi + \gamma\left|\psi\right|^2\psi = \mu\psi\ . \tag{3}$$

Equation (3) is supplemented with the boundary conditions: ψ tends to zero sufficiently fast as $|x|$ tends to infinity. The eigenvalue μ is referred to as the soliton propagation constant and its sign is adjusted depending on the signs of β and γ. We note that Eq. (3) in the presence of an external periodic potential has been studied in both one and two spatial dimensions [52, 53]. To determine the eigenfunction and eigenvalue pair (ψ, μ) we numerically integrate Eq. (3) using the spectral renormalization method [54] (see details in Appendix A). It is worth mentioning that a special solution for Eq. (3) is known to exist for $\beta > 0, \gamma = +1$ and is given by [55]

$$\psi(x) = \sqrt{\frac{3}{40\beta}}\ \mathrm{sech}^2\left(\frac{x}{\sqrt{40\beta}}\right)\ , \quad \mu = \frac{1}{25\beta}\ . \tag{4}$$

In Figs. 1 and 2 we show typical examples of nonlinear mode profiles (solutions of Eq. (3)) for both positive and negative values of β, γ and μ. First, we address the positive β case of which three different solutions corresponding to different soliton eigenvalues μ are depicted in Fig. 1. It is seen that the soliton amplitude becomes larger as μ increases, and as a result the soliton profile becomes more localized. The soliton shown in Fig. 1(a) corresponds to analytical solution (4) for $\beta = 1/10$. It is interesting to note that the soliton shapes given in Figs. 1(b) and 1(c) display a weak oscillatory tail and in some space domains become negative. This is contrary to the analytical solution in Eq. (4) which is postive-definite and monotonically decaying as x approaches $\pm\infty$. We can understand this oscillatory feature by examining the large x asymptotics of Eq. (3) given by

$$\frac{1}{2}\partial_x^2\psi - \beta\partial_x^4\psi \approx \mu\psi\ . \tag{5}$$

Making the ansatz $\psi(x) \sim \exp(sx)$ we find nontrivial solutions for values of the exponent s satisfying

$$s = \pm\left(\frac{1}{4\beta}\left(1 \pm \sqrt{1 - 16\beta\mu}\right)\right)^{1/2}\ . \tag{6}$$

It is evident that the exponent s is real when $\beta = 1/10$ and $\mu = 2/5$, whereas it becomes complex for $\mu = 2$ and 4. This explains the oscillatory behavior of the soliton tails.

Next, consider the negative β case which appears to be profoundly different. As noted in [56] and [57] there are no localized solutions to Eq. (3) for positive γ and μ. Thus we limit ourselves to the case where $\gamma = -1$ and negative μ values. With this in mind, we show in Fig. 2 typical

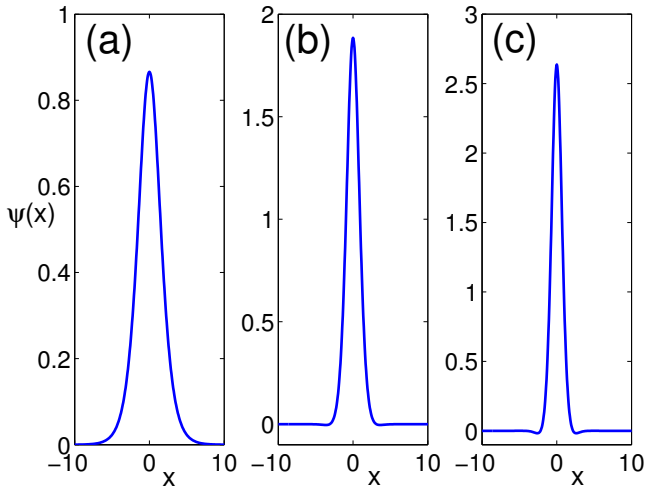

Figure 1: Line soliton solutions to Eq. (3) for $\beta = 0.1, \gamma = +1$ and soliton eigenvalues $\mu = 0.4$(a), 2(b) and 4(c).

solutions for various soliton eigenvalues. As one notices, the soliton profiles show a drastic difference in comparison to their $\beta > 0$ counterparts in the sense that they become highly oscillatory. Having found nonlinear modes for various sets of model parameters we turn our attention next to the question of linear stability analysis.

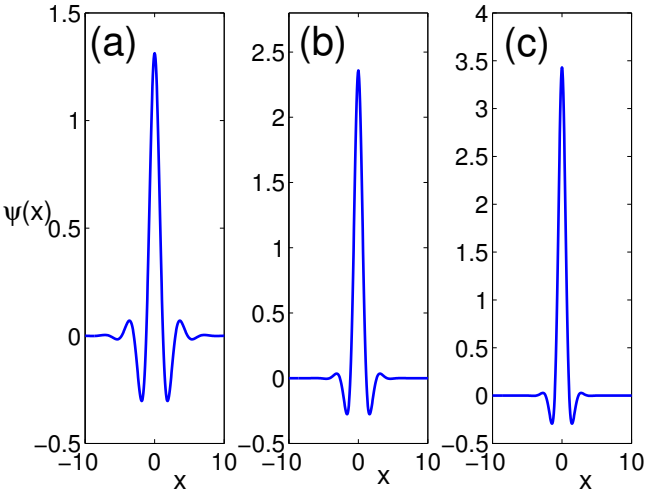

Figure 2: Same as in Fig. 1, but for parameters $\beta = -0.1, \gamma = -1$ and soliton eigenvalues $\mu = -1.5$(a), -4(b) and -8(c).

3. Linear stability analysis

To study the linear stability of the line soliton solutions found above, we write a weakly perturbed solution of Eq. (1) in the form

$$\phi(x, y, t) = [\psi(x) + \varepsilon\eta(x, y, t)]\, e^{i\mu t} \,, \tag{7}$$

where $|\varepsilon| \ll 1$ is a dimensionless parameter used to measure the strength of the perturbation and η is a complex transverse perturbation that depends on x, y and t. Note that we are considering here the linear stability of a real-valued wave function ψ. Substituting the ansatz (7) into Eq. (1) we find to order ε

$$i\eta_t - \mu\eta + \frac{1}{2}\Delta\eta - \beta\Delta^2\eta + \gamma\psi^2\,(2\eta + \eta^*) = 0 \,. \tag{8}$$

Equation (8) is a linear constant coefficient in y and t (and variable in x) PDE that governs the evolution of the perturbation η subject to the following boundary conditions: $\eta \to 0$ as $|x| \to \infty$ sufficiently fast and periodic in y. With this in mind, we decompose the perturbation in terms of its Fourier modes and assume that the time evolution is exponential

$$\eta(x, y, t) = f_q(x)e^{i(qy+\omega(q)t)} + g_q^*(x)e^{-i(qy+\omega^*(q)t)} \,, \tag{9}$$

where f_q, g_q are the perturbation Fourier modes assumed to be localized in x with corresponding wavenumber q and complex frequency $\omega(q)$ that measures the perturbation growth rate. Substituting the anstatz (9) into Eq. (8) and collecting terms proportional to $\exp(i(qy + \omega t))$ and $\exp(-i(qy + \omega^* t))$ independently results in the following non-Hermitian eigenvalue system

$$\begin{pmatrix} 0 & \mathbb{M}_{12} \\ \mathbb{M}_{21} & 0 \end{pmatrix} \begin{pmatrix} F_q \\ G_q \end{pmatrix} = \omega \begin{pmatrix} F_q \\ G_q \end{pmatrix} \,, \tag{10}$$

where, by definition, $F_q = f_q + g_q, G_q = f_q - g_q$ and the off-diagonal elements are

$$\mathbb{M}_{21} = \mathbb{L}_1 - q^2/2 - \beta q^4 + 2\beta q^2\partial_x^2 \,, \tag{11}$$
$$\mathbb{M}_{12} = \mathbb{L}_2 - q^2/2 - \beta q^4 + 2\beta q^2\partial_x^2 \,, \tag{12}$$

for

$$\mathbb{L}_1 = -\mu + \partial_x^2/2 - \beta\partial_x^4 + 3\gamma\psi^2 \,, \tag{13}$$
$$\mathbb{L}_2 = -\mu + \partial_x^2/2 - \beta\partial_x^4 + \gamma\psi^2 \,. \tag{14}$$

Note that the linear operators $\mathbb{L}_1$ and $\mathbb{L}_2$ are self-adjoint with respect to the standard $L^2(\mathbb{R})$ real-valued inner product

$$\langle u_1, u_2\rangle_{L^2(\mathbb{R})} = \int_{\mathbb{R}} u_1 u_2 \; dx \,, \tag{15}$$

which induces the norm

$$||u||_2 = \left(\int_{\mathbb{R}} u^2(x) \; dx\right)^{1/2} \,. \tag{16}$$

It is obvious from Eq. (9) that for a fixed wavenumber q, the eigenvalue $\omega = \omega(q)$ with nonzero imaginary component will grow exponentially in time, hence the perturbation η becomes unbounded. In this case, we say that the nonlinear mode $\phi(x, y, t) = \psi(x, \mu)\exp(i\mu t)$ is linearly unstable to transversally modulated perturbations. To determine if such modes are indeed linearly stable or not we

solve eigenvalue problem (10) and compute the spectrum ω as a function of the transverse wavenumber q. This is accomplished by numerically approximating the second and fourth-order derivatives ∂_x^2 and ∂_x^4 using, for example, spectral or finite difference differentiation matrices on a large computational domain [58]. The imaginary part of the eigenvalue $\omega(q)$ (corresponding to TI) is shown in Fig. 3 for $\beta = 1/10, \gamma = +1$ and various values of the transverse wavenumber q. The solid, dashed and dashed-dotted curves correspond to different soliton eigenvalues μ whose shapes are depicted in Fig. 1. The numerical results reveal the existence of a finite band $\mathcal{I} = (0, q_{\rm cut}(\mu, \beta))$ of Fourier modes that grow exponentially in time and force the soliton to disintegrate (see Sec. 6 for detailed numerical simulations). The numerical findings suggest that the measure of the interval $\mathcal{I}$ is a monotonic function of μ. Importantly, the instability develops for any small wavenumber q and attains its maximum value Im $\omega_{\rm max} \equiv \max_q$ Im $(\omega(q))$ at some wavenumber $q_{\rm max}$. We note that large soliton amplitudes experience the fastest instability development. The linear stability analysis suggests that the line soliton is stable against short wavelength transverse perturbations (see Sec. 6).

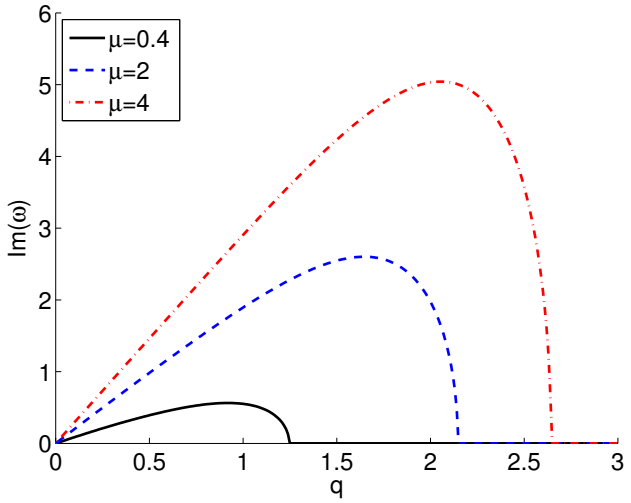

Figure 3: The imaginary part of the spectrum numerically generated by solving eigenvalue problem (10) with parameters $\beta = 0.1, \gamma = +1$ and several eigenvalues μ. The solid, dashed, and dashed-dotted curves correspond to the three solutions shown in Fig. 1.

In order to understand the role of the biharmonic dispersion coefficient β in the development of TI we have repeated the above numerical experiments for larger values of β. The main characteristics of the instability pattern remain unchanged with the slight exception that the unstable band measure shrinks and the maximum unstable eigenvalue decreases (see Fig. 4). Hence a sizable instability pattern is observed on longer time scales. As an example, for fixed $\mu = 4, \gamma = +1$ we find for $\beta = 0.1$ that $q_{\rm cut} \approx 2.65$ and Im $\omega_{\rm max} \approx 5.04$ at $q_{\rm max} \approx 2.06$. Compare this with $\beta = 0.25$ where $q_{\rm cut} \approx 2.17$ and Im $\omega_{\rm max} \approx 4.87$ is located at $q_{\rm max} \approx 1.71$. This result is somehow not so surprising since for positive β the operator $\Delta - \beta\Delta^2$ produces larger effective dispersion than the Laplacian alone, hence it tends to weaken, but not eliminate, the instability.

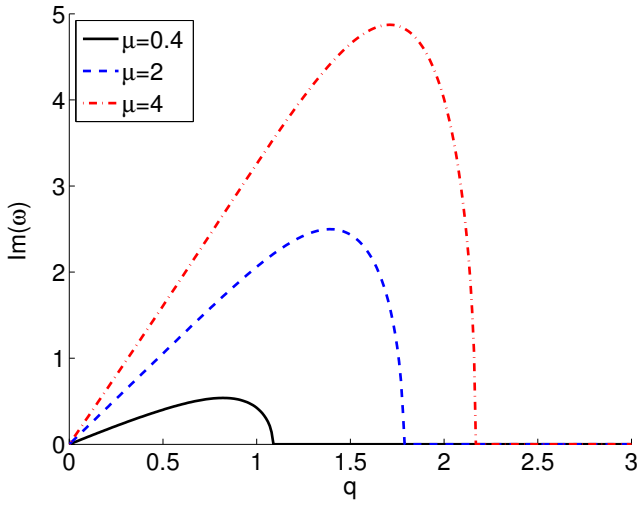

Figure 4: Numerically generated transverse instability growth rates for $\beta = 0.25, \gamma = +1$ and various soliton eigenvalues μ.

Next we proceed with the negative β case. As before, system (10) is solved numerically for the perturbation eigenvalues $\omega(q)$ with negative values of γ and μ. In sharp contrast to what we have so far observed, the unstable linear spectrum Im $\omega(q)$ with relatively small soliton eigenvalues $|\mu|$ are now compactly supported on the interval $\mathcal{I}_q = (q_{\rm cut}^{(1)}(\beta, \mu), q_{\rm cut}^{(2)}(\beta, \mu))$. Moreover, the linear stability analysis predicts that long wavelength transverse perturbations do not grow exponentially in time. The length of this *instability island* $\mathcal{I}_q$ expands with increasing soliton eigenvalue $|\mu|$. The numerical results seem to suggest that higher amplitude solitons are more susceptible to instability against long wavelength perturbations. For fixed nonlinearity coefficient γ and soliton eigenvalue μ, larger $|\beta|$ values have little effect on the overall nature of the spectrum, as one sees in Fig. 6.

4. Asymptotic analysis: long wavelength limit

To support our numerical findings we resort in this section to perturbation theory and derive an asymptotic formula for the perturbation eigenvalues $\omega(q)$ valid in the long wavelength limit, i.e. $q \to 0$. We start by expanding the perturbation eigenfunctions F_q and G_q as well as the eigenvalues $\omega(q)$ in an asymptotic series for small q:

$$\omega = q\omega_1 + q^2\omega_2 + \cdots \tag{17}$$

$$F_q(x) = F_0(x) + qF_1(x) + q^2F_2(x) + \cdots \tag{18}$$

$$G_q(x) = G_0(x) + qG_1(x) + q^2G_2(x) + \cdots \tag{19}$$

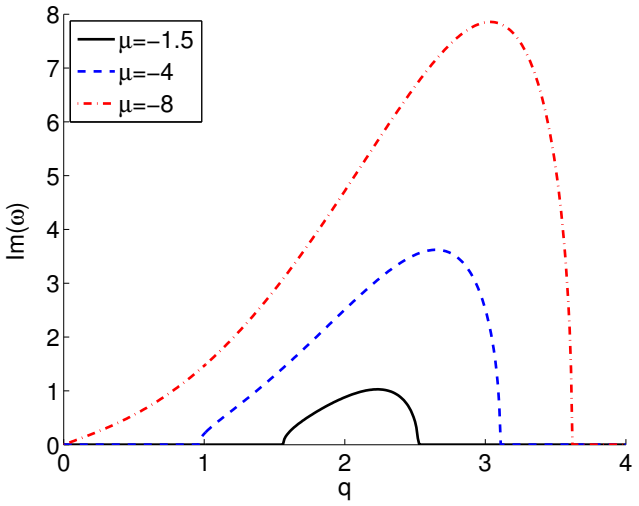

Figure 5: Same as Fig. 3, but for $\beta = -0.1, \gamma = -1$ and a few eigenvalues μ. The three curves correspond to the three solutions shown in Fig. 2.

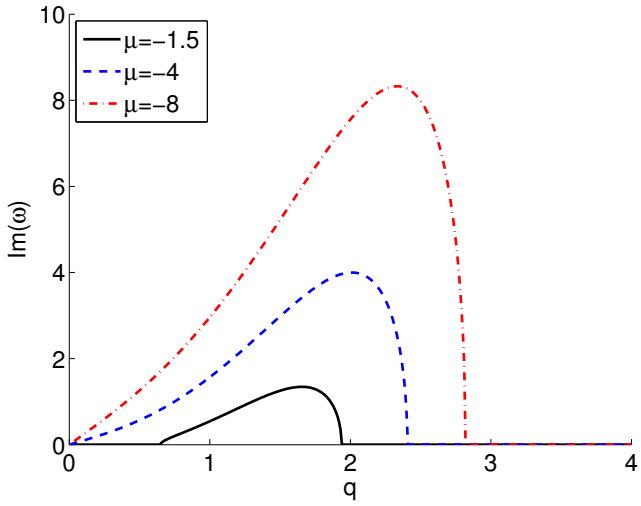

Figure 6: Imaginary part of the eigenvalue spectrum for system (10) computed numerically with parameters $\beta = -0.25, \gamma = -1$ and several eigenvalues μ.

Substituting expansions (17)-(19) into boundary value problem (10) and collecting terms at each order of q we find

$$O(1): \quad \mathbb{L}_1 F_0 = 0\,, \qquad \mathbb{L}_2 G_0 = 0\,, \tag{20}$$

$$O(q): \quad \mathbb{L}_1 F_1 = \mathcal{P}_1^F\,, \qquad \mathbb{L}_2 G_1 = \mathcal{P}_1^G\,, \tag{21}$$

$$O(q^2): \quad \mathbb{L}_1 F_2 = \mathcal{P}_2^F\,, \qquad \mathbb{L}_2 G_2 = \mathcal{P}_2^G\,, \tag{22}$$

and in general for any order $n \geq 3$

$$O(q^n): \quad \mathbb{L}_1 F_n = \mathcal{P}_n^F\,, \qquad \mathbb{L}_2 G_n = \mathcal{P}_n^G\,, \tag{23}$$

where the functions $\mathcal{P}_n^F$ and $\mathcal{P}_n^G$ depend on the previous F_l and G_l for $l = 0, \ldots, n-1$. As mentioned above, all the eigenfunctions F_n and G_n are assumed to be smooth and belong to the space of square integrable functions defined on the whole real line. Our aim is to solve Eqns. (20)-(22) successively. Since Eq. (1) admits gauge and space-translation invariance symmetries it follows

$$\mathbb{L}_1\left(\partial_x \psi\right) = 0\,, \quad \mathbb{L}_2\left(\psi\right) = 0\,. \tag{24}$$

Relation (24) combined with the asymptotic result in Eq. (6) imply that the dimension of the kernel (in $L^2(\mathbb{R})$) of $\mathbb{L}_j, j = 1, 2$ is at most two. We have numerically solved the eigenvalue problems $\mathbb{L}_1 v_1 = \lambda_1 v_1$ and $\mathbb{L}_2 v_2 = \lambda_2 v_2$ by representing each derivative by its corresponding finite-difference or spectral differentiation matrix with zero Dirichlet boundary conditions on a sufficiently large spatial domain and collocating the function $\psi^2(x)$ along the matrix diagonal. Our numerical findings strongly indicate that the only eigenfunctions of $\mathbb{L}_1$ and $\mathbb{L}_2$ that belong to the $L^2(\mathbb{R})$ space, with corresponding zero eigenvalues, are precisely those functions satisfying (24). With this at hand, we shall therefore assume throughout the rest of this paper that there exists $\{\beta_0, \mu_0, \gamma_0\}$ for which the dimension of the kernel of $\mathbb{L}_j, j = 1, 2$ is exactly one. Under the above assumption, we write the homogenous solution to Eq. (20) as $F_0 = C_1 \partial_x \psi$ and $G_0 = C_2 \psi$ for nonzero constants C_1 and C_2. At order q, we have $\mathcal{P}_1^F = \omega_1 G_0$ and $\mathcal{P}_1^G = \omega_1 F_0$. Differentiating Eq. (3) with respect to μ we find $F_1 = C_2 \omega_1 \partial_\mu \psi$. By the Fredholm Alternative theorem, an $L^2(\mathbb{R})$ solution to $\mathbb{L}_2 G_1 = \mathcal{P}_1^G$ exists and is given by $G_1 = C_1 \tilde{\psi}$ such that $\mathbb{L}_2 \tilde{\psi} = \omega_1 \partial_x \psi$ (up to a homogenous solution). At order q^2, we have $\mathcal{P}_2^F = C_1 \omega_1 \tilde{\psi} + C_2 \omega_2 \psi + C_1 \partial_x \psi/2 - 2\beta C_1 \partial_x^2 (\partial_x \psi)$ and $\mathcal{P}_2^G = C_2 \omega_1^2 \partial_\mu \psi + C_1 \omega_2 \partial_x \psi + C_2 \psi/2 - 2\beta C_2 \partial_x^2 \psi$. The solvability condition

$$\langle \psi, \mathcal{P}_2^G \rangle_{L^2(\mathbb{R})} = 0\,, \tag{25}$$

gives the following expression for the perturbation spectrum

$$\omega = \pm i q \Omega^{1/2} + O(q^2)\,, \tag{26}$$

where

$$\Omega = \frac{4\beta \left|\left|\partial_x \psi\right|\right|_2^2 + \left|\left|\psi\right|\right|_2^2}{\partial_\mu \left|\left|\psi\right|\right|_2^2}\,. \tag{27}$$

Thus for positive β the numerator in Eq. (27) is positive-definite, hence all solitary wave solutions to Eq. (3) satisfying the condition $\partial_\mu \left|\left|\psi\right|\right|_2^2 > 0$ are unstable against transverse perturbations with large wavelength and as a result grow exponentially in time. On the other hand, for negative β all transverse perturbations with wavenumbers satisfying $|q| \ll 1$ remain bounded for short time scales if $\left|\left|\psi\right|\right|_2^2 > -4\beta \left|\left|\partial_x \psi\right|\right|_2^2$ and $\partial_\mu \left|\left|\psi\right|\right|_2^2 < 0$.

To confirm result (26) we have compared it with the numerically computed TI eigenvalues for $\beta = 1/10, \gamma = +1$ and various soliton eigenvalues. The quantity $\partial_\mu ||\psi||_2^2$ is

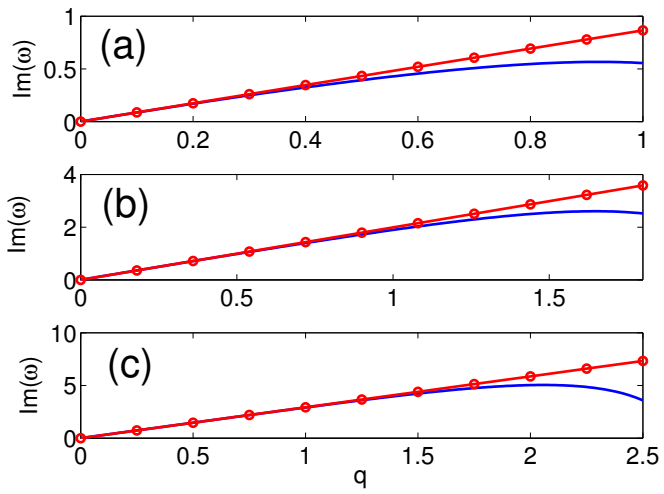

Figure 7: The imaginary part of the TI spectrum computed from Eq. (26) (circles) and by numerical solution of eigenvalue problem (10) (solid line) for $\beta = 0.1$ and $\gamma = +1$. The panels correspond to solution eigenvalues $\mu = 0.4$(a), 2(b) and 4(c). The approximate slopes $\Omega^{1/2}$ are 0.866(a), 1.992(b) and 2.931(c).

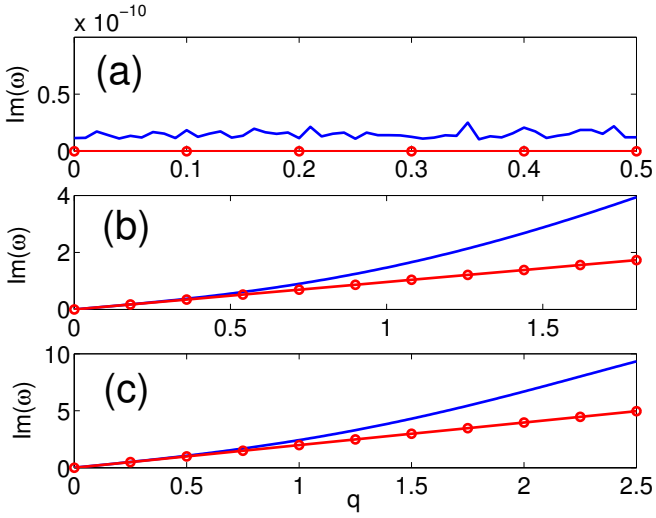

Figure 8: Same as Fig. 7, but for $\beta = -0.1$ and $\gamma = -1$. The panels correspond to solution eigenvalues $\mu = -4$(a), -8(b) and -12(c). The approximate slopes $\Omega^{1/2}$ are 0(a), 0.962(b), and 1.984(c).

computed using a centered finite differences stencil. A summary of the findings are shown in Fig. 7. For small wavenumbers q, Eq. (26) agrees well with the numerically generated perturbation eigenvalues (see Table 1 in Sec. 5). For the parameter regime considered here, $\partial_\mu ||\psi||_2^2$ is always positive. Similar tests have been performed for negative β values. In particular, for small soliton eigenvalues $|\mu|$ we find that the term $4|\beta|\,||\partial_x\psi||_2^2$ is smaller than $||\psi||_2^2$ and $\partial_\mu ||\psi||_2^2 < 0$, hence ω is real and the soliton is linearly stable (see Fig. 8(a)). On the other hand, as $|\mu|$ increases $4|\beta|\,||\partial_x\psi||_2^2$ grows larger than $||\psi||_2^2$ and the perturbation eigenvalues become purely complex (linearly unstable) for small q (see Figs. 8(b) and 8(c)).

5. Variational formulation

The previous approaches to compute the transverse dispersion relation $\omega(q)$ were based on numerical integration of boundary eigenvalue problem (10) as well as on the asymptotic analysis valid for small wavenumbers. In this section we take a different approach to compute and study the development of the spectral instability using a variational formulation. The central idea behind the method is to reformulate Eq. (1) in terms of its corresponding Lagrangian functional, then make a suitable solution ansatz that depends on few degrees of freedom and obtain an effective Lagrangian by integrating over a reduced number of degrees of freedom. By taking the variational derivative of the reduced Lagrangian, we obtain a coupled set of PDEs that are later used to study perturbation theory. We remark that this variational approach has been used to obtain approximate analytical forms for solitons in various settings [59, 60, 61].

We begin by considering the Lagrangian functional

$$\mathcal{L} = \frac{1}{2}\iiint_{\mathbb{R}^2\times[0,T]} \mathcal{G}\; dxdydt\;, \tag{28}$$

$$\mathcal{G} = i\,(\phi\partial_t\phi^* - \phi^*\partial_t\phi) + |\nabla\phi|^2 + 2\beta|\Delta\phi|^2 - \gamma|\phi|^4\;, \tag{29}$$

that using the Euler-Lagrange equations with the respect to the solution $\phi(x, y, t)$ reproduces Eq. (1). Our strategy for computing the transverse instability dispersion curves is as follows. First, let $\varphi_\mu(x)$ be a smooth and real-valued localized solution to Eq. (3) corresponding to eigenvalue μ. Multiplying that equation by $\varphi_\mu(x)$ and integrating over the whole real line gives

$$\gamma||\varphi_\mu||_4^4 = \mu||\varphi_\mu||_2^2 + \frac{1}{2}||\partial_x\varphi_\mu||_2^2 + \beta||\partial_x^2\varphi_\mu||_2^2\;, \tag{30}$$

where we define the $L^p(\mathbb{R})$ norm of φ_μ by

$$||\varphi_\mu||_p = \left(\int_{\mathbb{R}} (\varphi_\mu)^p\; dx\right)^{1/p}\;. \tag{31}$$

We now make the ansatz solution to Eq. (1) that is a one-dimensional soliton modulated in the transverse y-direction i.e.

$$\phi^A(x, y, t) = A(t, y)\varphi_\mu(x)e^{i\mu t}\;, \tag{32}$$

where A is a complex-valued amplitude that depends on y and t. This separation of variables approach, where the trial function $\varphi_\mu(x)$ is kept exact, simplifies the calculations and allows one to relate back to the stability problem by choosing the amplitude A to depend on t and y only. Also, in the method proposed here, the solution $\varphi_\mu(x)$ is either known analytically, as is the case in Eq. (4), or may

be numerically generated. A more general ansatz ϕ^A that includes more parameters (e.g. soliton width and phase) is possible (see [62] for the classical NLS equation). This could lead to better approximations for the perturbation eigenvalue ω, however the analysis could become cumbersome. The nice thing about our ansatz is that it simplifies the calculations, captures the structure of the unstable spectrum and agrees well with the previous approaches.

Substituting (32) into the Lagrangian (28) and integrating the x degree of freedom we obtain the effective Lagrangian

$$L_{\text{eff}}\left(A, A^*\right) = \frac{1}{2}\int_{\mathbb{R}} \mathcal{G}(\phi, \partial_t\phi, \nabla\phi, \Delta\phi)\Big|_{\phi=\phi^A} dx \ , \quad (33)$$

that after some calculations simplifies to

$$\begin{aligned} L_{\text{eff}}(A, A^*) = & \frac{i}{2}\left(A\partial_t A^* - A^*\partial_t A\right)E_1 + \mu|A|^2E_1 \quad (34)\\ & + \frac{1}{2}|A|^2E_2 + \frac{1}{2}|\partial_y A|^2E_1 + \beta|A|^2E_3 \\ & - \beta\left(A^*\partial_y^2 A + A\partial_y^2 A^*\right)E_2 + \beta|\partial_y^2 A|^2E_1 \\ & - \frac{\gamma}{2}|A|^4E_4 \ , \end{aligned}$$

where $E_j, j = 1, 2, 3, 4$ are positive constants that implicitly depend only on β, γ and μ

$$E_1 = \int_{\mathbb{R}} \varphi_\mu^2 \ dx \ , \quad (35)$$

$$E_2 = \int_{\mathbb{R}} \left(\partial_x\varphi_\mu\right)^2 \ dx \ , \quad (36)$$

$$E_3 = \int_{\mathbb{R}} \left(\partial_x^2\varphi_\mu\right)^2 \ dx \ , \quad (37)$$

$$E_4 = \int_{\mathbb{R}} \varphi_\mu^4 \ dx \ . \quad (38)$$

To obtain the dynamical equation that governs the evolution of the amplitude A, we use the first variation principle $\delta\mathcal{L} = 0$ via the Euler-Lagrange equation

$$\frac{\partial L_{\text{eff}}}{\partial A^*} - \frac{\partial}{\partial t}\frac{\partial L_{\text{eff}}}{\partial(\partial_t A^*)} - \frac{\partial}{\partial y}\frac{\partial L_{\text{eff}}}{\partial(\partial_y A^*)} + \frac{\partial^2}{\partial y^2}\frac{\partial L_{\text{eff}}}{\partial(\partial_y^2 A^*)} = 0 \ . \quad (39)$$

A straightforward calculation gives

$$\begin{aligned} & i\partial_t A - \left(\mu + \frac{E_2}{2E_1} + \beta\frac{E_3}{E_1}\right)A + \left(\frac{1}{2} + 2\beta\frac{E_2}{E_1}\right)\partial_y^2 A \quad (40)\\ & \quad - \beta\partial_y^4 A + \gamma\frac{E_4}{E_1}|A|^2 A = 0 \ . \end{aligned}$$

With this result at hand, we next proceed with the question of stability. Note that $A = 1$ is a fixed-point of Eq. (40) which implies that φ^A is an exact solution to Eq. (3). A small perturbation around the steady and homogenous state in the form

$$A(t, y) = 1 + \varepsilon A_1(t, y) + \cdots \ , \quad \varepsilon \ll 1 \ , \quad (41)$$

can be interpreted as a perturbation of the soliton φ_μ. Since, in this case, Eq. (32) reads $\phi^A(x, y, t) = [\varphi_\mu(x) + \varepsilon A_1(t, y)\varphi_\mu(x) + \cdots]\exp(i\mu t)$, $A_1\varphi_\mu$ can be thought of as transverse perturbation η. Substituting the asymptotic expansion (41) into Eq. (40) one finds to leading order in ε

$$\gamma E_4 = \mu E_1 + \frac{1}{2}E_2 + \beta E_3 \ , \quad (42)$$

which is identical to Eq. (30). At order ε we find the following linear evolution equation

$$i\partial_t A_1 + \left(\frac{1}{2} + \frac{2\beta E_2}{E_1}\right)\partial_y^2 A_1 - \beta\partial_y^4 A_1 + \frac{\gamma E_4}{E_1}\left(A_1 + A_1^*\right) = 0 \ . \quad (43)$$

Next we seek a plane wave solution to Eq. (43) with constant (in t and y) amplitudes u_q, v_q, wavenumbers $q \in \mathbb{R}$ and (in general) complex frequency ω that depends on q

$$A_1(t, y) = u_q \ e^{i(qy+\omega t)} + v_q^* \ e^{-i(qy+\omega^* t)} \ , \quad (44)$$

which upon substituting into Eq. (43) results in the non-Hermitian eigenvalue problem

$$\begin{pmatrix} 0 & \mathbb{W}_{12} \\ \mathbb{W}_{21} & 0 \end{pmatrix}\begin{pmatrix} U_q \\ V_q \end{pmatrix} = \omega\begin{pmatrix} U_q \\ V_q \end{pmatrix} \ . \quad (45)$$

Here we define $U_q = u_q - v_q, V_q = u_q + v_q$ and

$$\mathbb{W}_{12} = \frac{2\gamma E_4}{E_1} - \left(\frac{1}{2} + \frac{2\beta E_2}{E_1}\right)q^2 - \beta q^4 \ , \quad (46)$$

$$\mathbb{W}_{21} = -\left(\frac{1}{2} + \frac{2\beta E_2}{E_1}\right)q^2 - \beta q^4 \ . \quad (47)$$

The advantage of this variational approach over the one presented in Sec. 3 is that eigenvalue system (45) is exactly solvable, unlike the one given in Eq. (10) where only numerical diagonalization and long wavelength perturbation analysis is available. Solving for the eigenvalue ω gives the dispersion relation

$$\begin{aligned} \omega^2 = \ & q^2\left[\left(\frac{1}{2} + 2\beta\theta_1\right) + \beta q^2\right] \quad (48)\\ & \times\left\{\left(\frac{1}{2} + 2\beta\theta_1\right)q^2 + \beta q^4 - 2\gamma\theta_2\right\} \ , \end{aligned}$$

where $\theta_1 \equiv E_2/E_1$ and $\theta_2 \equiv E_4/E_1$ are positive constants. Furthermore, by letting $q_1 = \frac{1}{2\beta} + 2\theta_1$ and $K^2 = \frac{2\gamma\theta_2}{\beta}$ for $\beta \neq 0$ Eq. (48) is factored as

$$\omega^2 = \beta^2 q^2\left(q^2 + q_1\right)\left(q^2 - q_2^2\right)\left(q^2 + q_3^2\right) \ . \quad (49)$$

Here we define

$$q_2^2 = \frac{-q_1 + \sqrt{q_1^2 + 4K^2}}{2} \ , \quad (50)$$

with q_3^2 a positive quantity that depends on q_1 and K^2. Since $\gamma\beta > 0$ (the only case considered here) it follows

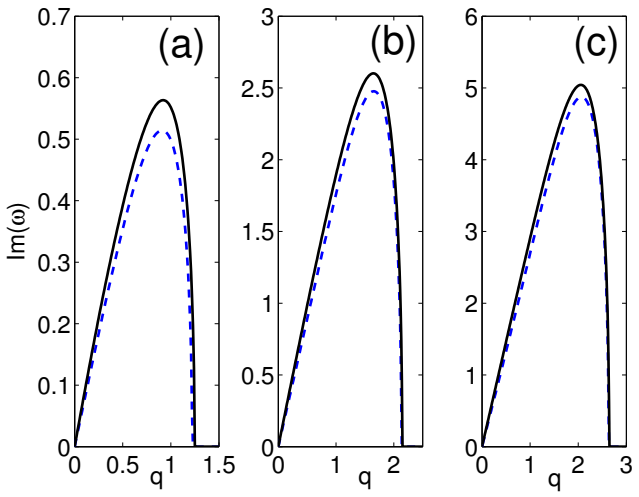

Figure 9: Instability growth rate obtained from Eq. (49) (dashed line) for $\beta = 0.1, \gamma = +1$ and eigenvalues $\mu = 0.4$(a), 2(b) and 4(c). The solid line is the numerically computed eigenvalues from system (10).

that K^2 is positive. Thus the soliton strip ψ is transversely unstable if $\omega^2 < 0$ and linearly stable otherwise. When β is positive it follows that $q_1 > 0$, in which case q_2^2 remain positive as well. This in turn implies the existence of a finite band of unstable Fourier modes $(0, q_2)$ for which Im ω is nonzero. This result is consistent with the numerical and perturbation findings obtained in Secs. 3 and 4. Figure 9 shows the instability growth rate Im ω as a function of the unstable modes q for typical parameters $\beta = 1/10$ and $\gamma = +1$. For comparison, we also show the numerically computed eigenvalues obtained by solving Eq. (10). As one can see, there is a relatively good qualitative agreement between the variational and numerical approaches. Both methods predict nearly identical unstable band measure, location of the most unstable mode $q_{\max}$, as well as maximum growth rates (with a slight difference from the numerical value Im $\omega_{\max}$ of about $8.7, 4.8, 3.3\%$ in Figs. 9 (a),(b),(c), respectively). In the long wavelength limit ($|q| \ll 1$), the perturbation growth rate is given by

$$\omega = \pm i q \Lambda^{1/2} + O(q^2) \ , \tag{51}$$

where

$$\Lambda = \gamma\theta_2 + 4\gamma\beta\theta_1\theta_2 \ . \tag{52}$$

Inspecting Eq. (52) the quantity Λ is positive, thus it leads to exponentially in time growing perturbations. Furthermore, it remarkably agrees with the asymptotically computed Ω given in Eq. (27). Table 1 shows typical values for $\Omega^{1/2}, \Lambda^{1/2}$ as well as the numerically generated slopes found from system (10) for different soliton propagation constants μ.

The situation for negative β proves to be much different than what we have so far encountered. This is most evident from the fact that q_1 can now be negative for some

μ	$\Omega^{1/2}$	$\Lambda^{1/2}$	Numerical
0.4	0.866	0.745	0.866
2	1.992	1.772	1.992
4	2.931	2.635	2.931

Table 1: Numerical values (rounded to the third digit) of $\Omega^{1/2}$ and $\Lambda^{1/2}$ obtained from formulas (27) and (52) for various soliton propagation constants. For comparison, we also show the numerically computed instability eigenvalues generated from eigenvalue problem (10) for $q = 0.01$. Parameters are $\beta = 0.1$ and $\gamma = +1$.

β. In this case, this leads to the formation of an otherwise nonexistent finite band of linearly stable modes followed by a measurable interval of unstable Fourier wavenumbers. This can be explained by noticing that for q^2 less than $-q_1 > 0$ the right-hand side of Eq. (49) is positive and switches signs ($\omega^2 < 0$) when q^2 lies in the interval $(-q_1, q_2^2)$. For fixed β, increasing the soliton eigenvalue $|\mu|$ forces the interval $(0, -q_1)$ to shrink to zero, hence the soliton becomes unstable for perturbations with small wavenumbers. The transition from a positive to a negative q_1 value occurs when $\theta_1 < -1/(4\beta)$ and is accompanied by the formation of a finite-size band of linearly stable modes ($\Lambda < 0$ for $\beta, \gamma < 0$). Thus there is an absence of a long wavelength instability. Interestingly enough, Ω becomes negative as well when $\theta_1 < -1/(4\beta)$, a surprising agreement with the asymptotic result discussed in Sec. 4 given the fact that we used a simple form for the variational ansatz. Finally, two typical examples corresponding to positive and negative q_1 values are shown in Fig. 10 for parameters $\beta = -1/10$ and $\gamma = -1$. Overall, we observe a good agreement between the numerically computed and semi-analytically obtained stable/unstable perturbation eigenvalues.

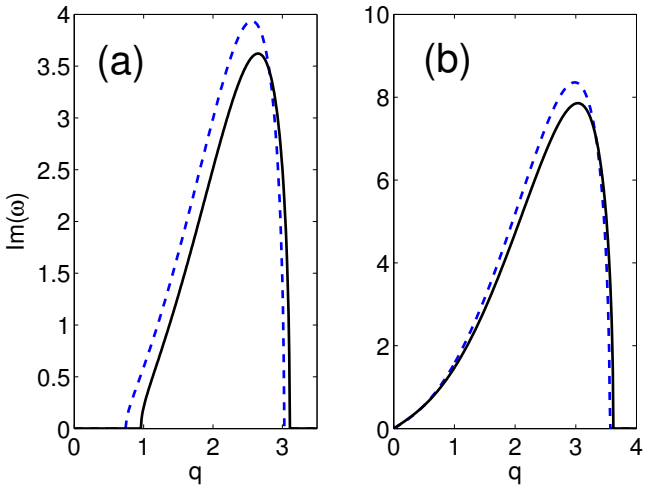

Figure 10: Same as Fig. 9, but for parameters $\beta = -0.1, \gamma = -1$ and eigenvalues $\mu = -4(a)$ and -8(b).

6. Direct numerical simulations

In this section we perform several direct numerical simulations to confirm the linear stability results obtained in Secs. 3,4 and 5 as well as report on the development of nonlinear instability. We have numerically solved the Cauchy problem associated with Eq. (1) using a fourth-order split-step integration method in time and Fourier spectral discretization in space with boundary conditions: ϕ decays rapidly to zero as $|x| \to \infty$ combined with periodic boundary conditions in the y-direction. The initial condition used in the simulations is

$$\phi(x, y, 0) = \psi(x) + \varepsilon \left[\partial_x \psi \cos(Qy) + i\psi \sin(Qy)\right] \ , \quad (53)$$

where $|\varepsilon| \ll 1$ and Q is the linear transverse perturbation wavenumber that corresponds to either a linearly stable or unstable mode. The form of the chosen perturbation is consistent with Eqs. (7) and (9).

First consider the positive β case. The dynamic evolution of a moderate amplitude soliton under the combined effects of a periodically modulated perturbation in the transverse y-direction and longitudinal localization is shown in Fig. 11. On a relatively short time scale, a neck-type instability develops (consistent with the linear theory - see Fig. 3) and ultimately leads to a full break up of the mode into a sequence of localized bright spots. The distance between adjacent filaments is approximately 4.19 units, which is roughly the period $(2\pi/Q)$ of the transverse perturbation. The long time fate of each individual filament is determined by its intensity: it will either self-focus, diffract or oscillate. To validate the linear stability results presented in Secs. 3 and 5 we repeat the numerical experiments, this time with wavenumber $Q > q_{\rm cut}$ corresponding to Im $\omega(Q > q_{\rm cut}) = 0$. As one can see from Fig. 12, for short times (linear stability regime) the wave pattern remains almost undisturbed compared to the initial state and develops weak bounded oscillations in the y-direction.

Next we shift our focus to the negative dispersion case ($\beta < 0$). Here we study nonlinear dynamics of transverse perturbations superimposed on top of a soliton stripe. The propagation constant μ is chosen such that the linear theory (asymptotic and variational) presented in Secs. 4 and 5 predicts the existence of three linear stable or unstable Fourier bands, which happens when $q_1 < 0$. With this at hand, we have simulated Eq. (1) with initial condition (53) for various values of Q residing in each linear stability/instability band. When Q falls into the stable linear band ($0 < Q^2 < -q_1$), full numerical simulations reveal that the soliton almost preserves its initial shape on the order of short time scale $1/\text{Im}\ \omega_{\max}(q) \approx 0.28$ (see Fig. 13). This observation seems to persist well beyond that time scale. On the other hand, for the same fixed q_1, but with Q^2 chosen now inside the interval $(-q_1, q_2^2)$ (corresponding to linearly unstable modes) the soliton experiences severe instability and eventually disintegrates into an array of well separated two-dimensional bright spots as shown in

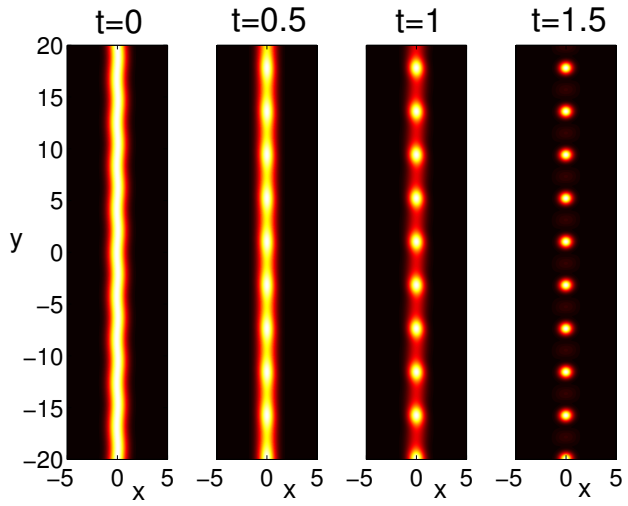

Figure 11: A snapshot top view of the intensity field $|\phi(x, y, t)|^2$ at various times obtained from numerical simulation of Eq. (1) using initial condition (53). The initial soliton profile $\psi(x)$ is chosen from Fig. 1(b) with parameters $\beta = 0.1, \mu = 2$ and $\gamma = +1$. The perturbation parameters are $\varepsilon = 0.05$ and $Q = 1.5$.

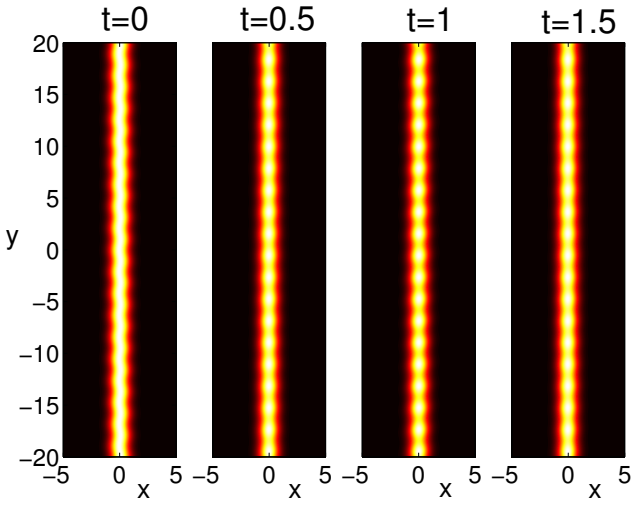

Figure 12: Same as Fig. 11, but with $Q = 3$.

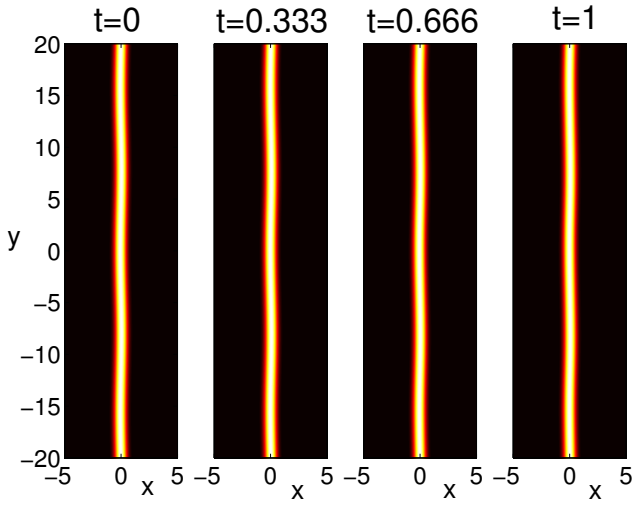

Figure 13: A snapshot top view of the intensity field $|\phi(x,y,t)|^2$ at various times obtained from numerical simulation of Eq. (1) using initial condition (53). The initial soliton profile $\psi(x)$ is chosen from Fig. 2(b) with parameters $\beta = -0.1, \mu = -4$ and $\gamma = -1$. The perturbation parameters are $\varepsilon = 0.05$ and $Q = 0.4$.

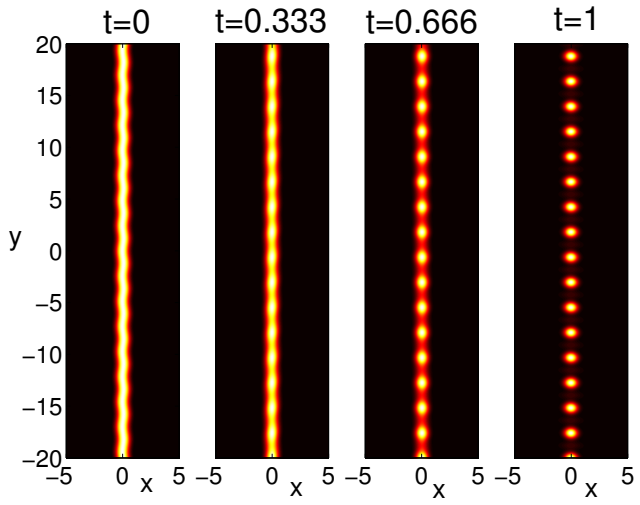

Figure 14: Same as Fig. 13, but with $Q = 2.6$.

Fig. 14. Perturbations with wavenumbers Q^2 belonging to the third linear stable band (q_2^2, ∞) were also examined and found to remain bounded up to $t = 1$, conferring with linear theory.

7. Conclusions

In this paper we have studied the dynamics and formation of coherent structures that result from the development of instabilities for families of one-dimensional localized waves due to the presence of transverse perturbation. Our model equation is the two-dimensional nonlinear Schrödinger equation in the presence of a fourth-order dispersion. The linear stability analysis predicts the existence of a finite band of unstable Fourier modes for which small transverse perturbations grow exponentially in time and lead to the break up of the soliton stripe. On time scales larger than the inverse of the growth rate Im $\omega_{\max}$ full nonlinear simulations reveal the formation of arrays of periodic two-dimensional filaments. The numerical linear stability analysis is supported by analytical results based on perturbation theory and variational Lagrangian model reduction.

Acknowledgements

The work of J.T.C. and Z.H.M was supported in part by NSF grant number DMS-0908599.

Appendix A. Spectral renormalization method

In this section we outline the spectral renormalization method [54] used to numerically construct soliton solutions. Other numerical methods based on functional optimization of Sobolev gradients [63] can also be implemented. Solutions to Eq. (3) are sought in the form $\phi(x,y,t) = ru(x)e^{i\mu t}$ where r is a yet to be determined renormalization factor and $u(x)$ is the real-valued mode profile satisfying

$$\frac{1}{2}\partial_x^2 u - \beta\partial_x^4 u + \gamma r^2 u^3 - \mu u = 0\,. \tag{A.1}$$

Multiplying Eq. (A.1) by u and integrating over the whole space gives

$$r^2 = \frac{\frac{1}{2}\left|\left|\partial_x u\right|\right|_2^2 + \beta\left|\left|\partial_x^2 u\right|\right|_2^2 + \mu\left|\left|u\right|\right|_2^2}{\gamma\left|\left|u\right|\right|_4^4}\,. \tag{A.2}$$

The function $u(x)$ is thus obtained by the following fixed-point iteration scheme

$$\hat{u}_{n+1} = \frac{\{\zeta - \mu\}\,\hat{u}_n + \gamma r_n^2 \mathcal{F}\left[u_n^3\right]}{\frac{1}{2}k^2 + \beta k^4 + \zeta}\,, \tag{A.3}$$

where $r_n^2 = r^2\big|_{u=u_n}$ and $\mathcal{F}, \mathcal{F}^{-1}$ are the forward and inverse Fourier transforms respectively defined by

$$\hat{f} = \mathcal{F}[f] = \frac{1}{\sqrt{2\pi}}\int_{\mathbb{R}} f(x)e^{-ikx}\,dx\,, \tag{A.4}$$

and

$$f = \mathcal{F}^{-1}\left[\hat{f}\right] = \frac{1}{\sqrt{2\pi}}\int_{\mathbb{R}} \hat{f}(k)e^{ikx}\,dk\,. \tag{A.5}$$

In iteration scheme (A.3) the parameter ζ is chosen such that $\zeta = \mu$ for $\beta > 0$ (in which case μ is also positive) and $\zeta < 0$ satsifying $1 < 16\beta\zeta$ when β is negative.

References

[1] A. Chen, M. Segev and D.N. Christodoulides, *Optical spatial solitons: historical overview and recent advances*, Rep. Prog. Phys., 75 (2012), 086401.

[2] Y.S. Kivshar and G.P. Agrawal, *Optical solitons*, Academic Press, (2003).
[3] M. Segev, *Optical spatial solitons*, Opt. Quant. Electron., 30 (1998), pp. 503-533.
[4] D.N. Christodoulides, F. Lederer and Y. Silberberg, *Discretizing light behaviour in linear and nonlinear waveguide lattices*, Nature, 424 (2003), pp. 817-823.
[5] F. Lederer, G.I. Stegeman, D.N. Christodoulides, G. Assanto, M. Segev and Y. Silberberg, *Discrete solitons in optics*, Phys. Rep., 463 (2008), pp. 1-126.
[6] M.J. Ablowitz, *Nonlinear dispersive waves: asymptotic analysis and solitons*, Cambridge University Press, (2011).
[7] E.A. Kuznetsov, A.M. Rubenchik and V.E. Zakharov, *Soliton stability in plasmas and hydrodynamics*, Phys. Rep., 142 (1986), pp. 103-165.
[8] P.G. Kevrekidis, D.J. Frantzesakakis and R. Carretero-Gonzalez, *Emergent Nonlinear Phenomena in Bose-Einstein Condensates*, Springer (2008).
[9] A.L. Hodgkin and A.F. Huxley, *A quantitative description of membrane current and its application to conduction and excitation in nerve*, J. Physiol. 117 (1952), pp. 500-544.
[10] A.S. Davydov and N.I. Kislukha, *Solitary excitons in one-dimensional molecular chains*, Physica Status Solidi (b), 59 (1973), pp 465-470.
[11] M.C. Cross and P.C. Hohenberg, *Pattern formation outside of equilibrium*, Phys. Rev. Mod. Phys., 65 (1993), pp. 851-1112.
[12] T.B. Benjamin and J.E. Feir, *The disintegration of wave trains on deep water*, J. Fluid Mech., 27 (1967), pp. 417-430.
[13] T. Taniuti and H. Washimi, *Self-trapping and instability of hydromagnetic waves along the magnetic field in a cold plasma*, Phys. Rev. Lett., 21 (1968), pp. 209-212.
[14] F.Kh. Abdullaev and J. Garnier, *Modulational instability of electromagnetic waves in birefringent fibers with periodic and random dispersion*, Phys. Rev. E, 60 (1999), pp. 1042-1050.
[15] C.K.R.T. Jones, R. Marangell, P.D. Miller, and R.G. Plaza, *Spectral and modulational stability of periodic wavetrains for the nonlinear Klein-Gordon equation*, J. Differential Equations, 257 (2014), pp. 4632-4703.
[16] K. Tai, A. Hasegawa and A. Tomita, *Observation of modulational instability in optical fibers*, Phys. Rev. Lett., 56 (1986), pp. 135-138.
[17] L. Salasnich, A. Parola and L. Reatto, *Modulational instability and complex dynamics of confined matter-wave solitons*, Phys. Rev. Lett., 91 (1986), 080405.
[18] R. Malendevich, L. Jankovic, G.I. Stegeman and J.S. Aitchison, *Spatial modulation instability in a Kerr slab waveguide*, Opt. Lett., 26 (2001), pp. 1879-1881.
[19] H. Fang, R. Malendevich, R. Schiek and G.I. Stegeman, *Spatial modulational instability in one-dimensional lithium niobate slab waveguides*, Opt. Lett., 25 (2000), pp. 1786-1788.
[20] D. Kip, M. Soljacic, M. Segev, E. Eugenieva and D.N. Christodoulides, *Modulation instability and pattern formation in spatially incoherent light beams*, Science, 290 (2000), pp. 495-498.
[21] J. Meier, G.I. Stegeman, D.N. Christodoulides, Y. Silberberg, R. Morandotti, H. Yang, G. Salamo, M. Sorel and J.S. Aitchison, *Experimental observation of discrete modulational instability*, Phys. Rev. Lett., 92 (2004), 163902
[22] Z.H. Musslimani, K.G. Makris, R. El-Ganainy and D.N. Christodoulides, *Optical solitons in PT periodic potentials*, Phys. Rev. Lett., 100 (2008), 030402.
[23] K.G. Makris, R. El-Ganainy, D.N. Christodoulides and Z.H. Musslimani, *Beam dynamics in Pt symmetric optical lattices*, Phys. Rev. Lett., 100 (2008), 103904.
[24] K.G. Makris, Z.H. Musslimani, D.N. Christodoulides and S. Rotter, *Constant-intensity waves and their modulation instability in non-Hermitian potentials*, arXiv:1503.08986, (2015).
[25] P.A.E.M. Janssen and J.J. Rasmussen, *Nonlinear evolution of the transverse instability of plane-envelope solitons*, Phys. Fluids, 26 (1983), pp. 6586-6587.
[26] Y.S. Kivshar and D.E. Pelinovsky, *Self-focusing and transverse instabilities of solitary waves*, Phys. Rep., 331 (2000), pp. 117-195.
[27] J.D. Carter and H. Segur, *Instabilities in the two-dimensional cubic nonlinear Schrödinger equation*, Phys. Rev. E, 68 (2003), 045601(R).
[28] V.E. Zakharov and A.M. Rubenchik, *Instability of waveguides and solitons in nonlinear media*, Sov. Phys. JETP, 38 (1974), pp. 494-500.
[29] A.V. Marmaev, M. Saffman, D.Z. Anderson, and A.A. Zozulya, *Propagation of light beams in anisotropic nonlinear media: From symmetry breaking to spatial turbulence*, Phys. Rev. A, 54 (1996), pp. 870-879.
[30] V. Tikhonenko, J. Christou, and B. Luther-Davies, *Three dimensional bright spatial soliton collision and fusion in a saturable nonlinear medium*, Phys. Rev. Lett., 76 (1996), pp. 2698-2701.
[31] M.A. Hoefer and B. Ilan, *Dark solitons, dispersive shock waves, and transverse instabilities*, Multiscale Model. Simul., 10 (2012), pp. 306-341.
[32] C. Anastassiou, M. Soljačić, M. Segev, E.D. Eugenieva, D.N. Christodoulides, D. Kip, Z.H. Musslimani, and J.P. Torres, *Eliminating the transverse instabilities of Kerr solitons*, Phys. Rev. Lett., 85 (2000), pp. 4888-4891.
[33] Z.H. Musslimani and J. Yang, *Transverse instability of strongly coupled dark-bright Manakov vector solitons*, Opt. Lett., 26 (2001), pp. 1981-1983.
[34] Z.H. Musslimani, M. Segev, A, Nepomnyashchy, and Y.S. Kivshar, *Suppression of transverse instabilities for vector solitons*, Phys. Rev. E, 60 (1999), pp. R1170-R1173.
[35] V.A. Brazhnyi and V.M. Pérez-García, *Stable multidimensional soliton stripes in two-component Bose-Einstein condensates*, Chaos Solitons Fractals, 44 (2011), pp. 381-389.
[36] Y. Kodama and M.J. Ablowitz, *Transverse instability of breathers in resonant media*, J. Math. Phys., 21 (1980), pp. 928-931.
[37] S.-P. Gorza, B. Deconinck, Ph. Emplit. T. Trogdon, and M. Haelterman, *Experimental demonstration of the oscillatory snake instability of the bright soliton of the (2+1)D hyperbolic nonlinear Schrödinger equation*, Phys. Rev. Lett., 106 (2011), 094101.
[38] D.E. Pelinovsky, E.A. Rouvinskaya, O.E. Kurkina, and B. Deconinck, *Short-wave transverse instabilities of line solitons of the two-dimensional hyperbolic nonlinear Schrödinger equation*, Theoret. Math. Phys., 179 (2014), pp. 452-461.
[39] Z.G. Chen, M. Segev, T.H. Coskun, D.N. Christodoulides, and Y.S. Kivshar, *Incoherently coupled dark-bright photorefractive solitons*, Opt. Lett., 21 (1996), pp. 1821-1823.
[40] Z.G. Chen, M. Segev, T.H. Coskun, and D.N. Christodoulides, *Observation of incoherently coupled photorefractive spatial soliton pairs*, Opt. Lett., 21 (1996), pp. 1436-1438.
[41] G. Fibich and B. Ilan, *Optical light bullets in a pure Kerr medium*, Opt. Lett., 29 (2004), pp. 887-889.
[42] D.N. Christodoulides and R.I. Joseph, *Femtosecond solitary waves in optical fibers-beyond the slowly varying approximation*, Appl. Phys. Lett., 47 (1985), pp. 76-78.
[43] A.B. Cavalcanti, J.C. Cruz, H.R. da Cruz and A.S. Gouveia-Neto, *Modulation instability in the region of minimum group-velocity dispersion of single-mode optical fibers via an extended nonlinear Schrödinger equation*, Phys. Rev. A, 43 (1991), pp. 6162-6165.
[44] S. Pitois and G. Millot, *Experimental observation of a new modulational instability spectral window induced by fourth-order dispersion in a normally dispersive single-mode optical fiber*, Opt. Comm., 226 (2003), pp. 415-422.
[45] K. Kitayama, K. Okamoto and H. Yoshinaga, *Extended four-photon mixing approach to modulational instability*, J. Appl. Phys., 64 (1988), pp. 1279-1287.
[46] F.Kh. Abdullaev, S.A. Darmanyan, S. Bischoff, P.L. Christiansen and M.P. Sorensen, *Modulational instability in optical fibers near the zero dispersion point*, Opt. Comm., 108 (1994), pp. 60-64.
[47] W. Hong, *Modulational instability of optical waves in the high*

dispersive cubic-quintic nonlinear Schrödinger equation, Opt. Comm., 213 (2002), pp. 172-182.
[48] A.G. Shagalov, *Modulational instability of nonlinear waves in the range of zero disperison*, Phys. Lett. A, 239 (1998), pp. 41-45.
[49] C.J. Pethick and H. Smith, *Bose-Einstein condensates in dilute gases*, Cambridge University Press, (2001).
[50] M.J. Ablowitz and H. Segur, *Solitons and the inverse scattering transform*, SIAM Press, (1981).
[51] J. Lega, J.V. Moloney and A.C. Newell, *Swift-Hohenberg equation for lasers*, Phys. Rev. Lett., 73 (1994), pp. 2978-2981.
[52] J.T. Cole and Z.H. Musslimani, *Band gaps and lattice solitons for the higher-order nonlinear Schrödinger equation with a periodic potential*, Phys. Rev. A, **90** (2014), 013815.
[53] J.T. Cole and Z.H. Musslimani, *Gap solitons and vortices for the two-dimensional biharmonic nonlinear Schrödinger equation with periodic potential*, in preparation (2015)
[54] M.J. Ablowitz and Z.H. Musslimani, *Spectral renormalization method for computing self-localized solutions to nonlinear systems*, Opt. Lett., 30 (2005), pp. 2140-2142.
[55] M. Karlsson and A. Höök, *Soliton-like pulses governed by fourth order dispersion in optical fibers*, Opt. Comm., 104 (1994), pp. 303-307.
[56] V.I. Karpman, *Influence of high-order dispersion on self-focusing. I. Qualitative investigation*, Phys. Lett. A, 160 (1991), pp. 531-537. *Influence of high-order dispersion on self-focusing. II. Numerical investigation*, Phys. Lett. A, 160 (1991), pp. 538-540.
[57] G. Fibich, B. Ilan, and G. Papanicolaou, *Self-focuing with fourth-order dispersion*, SIAM J. Appl. Math., 62 (2002), pp. 1437-1462.
[58] L.N. Trefethen, *Spectral Methods in MATLAB*, SIAM, Philadelphia (2000).
[59] B.A. Malomed, *Soliton management in periodic systems*, Springer, (2006).
[60] B.A. Malomed, *Variational methods in nonlinear fiber optics and related fields*, Progress in optics, 43 (2002), pp. 71-193.
[61] V.M. Pérez-García, H. Michinel, J.I. Cirac, M. Lewenstein and P. Zoller, *Dynamics of Bose-Einstein condensates: Variational solutions of the Gross-Pitaevskii equations*, Phys. Rev. A, 56 (1997), pp. 1424-1432.
[62] D. Anderson, A. Bondeson and M. Lisak, *Transverse instability of soliton solutions to nonlinear Schrödinger equations*, J. Plasma Phys., 21 (1979), pp. 259-266.
[63] J.J. Garcia-Ripoll and V.M. Pérez-García, *Optimizing Schrdinger functionals using Sobolev gradients: applications to quantum mechanics and nonlinear optics*, SIAM J. Sci. Comput., 23 (2001), pp. 1316-1334.